gels

Highly Porous Polyimide Gel for Use as Battery Separator with Room Temperature Ionic Liquid Electrolytes

Rocco P. Vigiano [1,*], James Wu [1], Daniel A. Scheiman [2], Brianne DeMattia [1], Patricia Loyselle [1], and Baochau N. Nguyen [2,*]

[1] NASA Glenn Research Center, 21000 Brookpark Road, Cleveland, OH 44135, USA
[2] Universities Space Research Associations/ E Street Technologies, NASA Glenn Research Center, 21000 Brookpark Road, Cleveland, OH 44135, USA
* Correspondences: rocco.p.viggiano@nasa.gov; baochau.n.nguyen@nasa.gov

Abstract

Advanced aerospace vehicular concepts require advances in many existing technologies, including space power and energy storage systems. Batteries represent one of the major areas in need of improvement, both in terms of energy density and safety, with growing concerns over the fire safety of commercial lithium-ion batteries. This has prompted efforts to develop nonflammable battery components, namely the electrolyte and separator. Existing commercial lithium-ion batteries utilize polyolefin microporous membranes as separators with an electrolyte consisting of a lithium salt dissolved in a mixture of cyclic carbonate solvents. This separator/electrolyte combination has ionic conductivities in the range of 10^{-2} to 10^{-3} S/cm. However, the cyclic carbonate solvents are inherently flammable. Room-temperature ionic liquids (RTILs) appear to be a safer alternative. They offer good ionic conductivities and are inherently nonvolatile and nonflammable, giving them a safety advantage. However, many promising RTILs for battery electrolytes are not compatible with commercial polyolefin separator materials. Alternative separator materials, such as polyimides, are nonflammable and are capable of accepting RTILs into their structure. Polyimide gels, with a composition of 4,4′-oxydianiline, 3,3′,4,4′-tetracarboxylic dianhydride and cross-linked with Desmodur N3300A, possess an open-porous, fibrillar network architecture which offers a high degree of porosity (typically greater than 85% porosity) for lithium-ion transport and conduction, as well as good mechanical properties. Furthermore, these polyimide gels are compatible with selected imidazolium-based RTILs. Nonflammable separator/electrolyte systems with room-temperature conductivities in the range of 10^{-3} S/cm have been evaluated. It has been demonstrated that 1-ethyl-3-methylimidazolium bis(trifluoromethylsulfonyl)imide was the most promising among six RTILs screened, in terms of both ionic conductivity and constant current cycling.

Keywords: polyimide; polyimide aerogel; polyimide sol-gel; polyimide gel separator; room temperature ionic liquids; ionic conductivity.

Academic Editor: Firstname Lastname

Received: date
Revised: date
Accepted: date
Published: date

Citation: To be added by editorial staff during production.

1. Introduction

A separator is a critical component used in batteries. It is a membrane that maintains a fixed distance between the anode and cathode while permitting ionic transport. It is fabricated to be as thin as possible to ensure minimal contribution to the overall cell mass, thereby maximizing the specific energy achievable by the cell. Ideally, battery separators for lithium-based batteries should possess the following properties: chemical stability, a thickness of 1 mil or less, at least 40% porosity, mechanical strength, wettability for chosen electrolytes, and dimensional stability [1,2].

To date, inexpensive and commonly used separators are polyolefin in composition such as Celgard® (low melting point ~130 ºC), used in lithium-ion batteries [4]. Celgard® separators range in thickness from 20 to 25 μm. Polyolefin separators are typically used with electrolyte compositions including ethylene carbonate (EC), dimethyl carbonate (DMC) or propylene carbonate (PC), solvents suitable for both dissolving the lithium salt and wetting the polyolefin separator[5]. This separator/electrolyte combination exhibits ionic conductivities ranging from 1×10^{-3} S/cm to 1×10^{-2} S/cm at room temperature. However, polyolefin separators have melting points below the thermal runaway temperature of lithium-ion batteries, poor thermal stability and inherent flammability [6]. Efforts to improve the performance of separators by reducing flammability and shrinkage, while improving ionic conductivity, have been intensively investigated [7].

Several polymer substrates like polyacrylonitrile (PAN) and its composites [8–10] have been of interest due to their higher porosity (> 68%) and higher mechanical strength than most Celgard® separators (porosity > 45%) [1]. Other materials explored include poly(vinylidene fluoride) [11,12], the copolymer poly(methyl methacrylate)-poly(vinylidene fluoride) [13], poly(m-phenylene isophthalamide) [14] and poly(arylene ether nitrile) [15], for instance. While these materials exhibit improved properties, the carbonate-based electrolytes or wetting solvents still impose a flammability risk [6].

Room-temperature ionic liquids (RTILs) are another class of electrolytes considered as replacements for conventional carbonate-based electrolytes. RTILs are salt-like liquids composed of cations and anions that are molten at or near ambient temperature. Depending on the chemical structure and cation/anion type, RTILs can have viscosities up to ~860 cP at 20 °C [16,17]. They can exhibit high ionic conductivity (up to 10^{-2} S/cm) and wide electrochemical windows [18,19] and, more notably, they are known for being nonvolatile [20,21] and thermally stable above 200 ºC to 400 °C [22,23]. However, it has been found that several RTILs have poor wettability on polyolefin separators, largely due to the high contact angles at the RTIL/separator interface, which lowers the effective ionic conductivity [24,25]. Carbonate solvents such as ethylene carbonate or propylene carbonate have been added in an attempt to improve the wettability of RTILs [26,27].

Contact angle measurements for separators with improved wetting properties for RTILs have been widely investigated [24,25,28,29]. Research on electrospun polyacrylonitrile microfiber (PAN) separators has shown better wetting with 1-methyl-1-propylpyrrolidinium bis(trifluoromethylsulfonyl)imide (PYR13-TFSI) or 1-methyl-1-propylpyrrolidinium bis(fluorosulfonyl)imide (PYR13-FSI) (in 1:1 ethylene carbonate and diethyl carbonate) compared to Celgard polypropylene (PP) separators, due to their higher porosity, 83% vs. 39%, respectively [26]. A study conducted by Caimi et al [28] showed an improvement in contact angle when SiO_2 nanoparticles (10 wt%) were incorporated into

poly(vinylidene fluoride-co-hexafluoropropylene) (PVDF-HFP) in PYR1308b and sodium dodecyl sulfate was used as a wetting agent. The type of anion used, such as bis(trifluoromethanesulfonyl)imide ($TFSI^-$) or tetrafluoroborate (BF_4^-), also contributes to RTIL uptake [30]. Cheruvally et al [30] demonstrated that electrospun poly(vinylidene fluoride-co-hexafluoropropylene), PVDF-HFP, membranes could absorb 750% of 1-butyl-3-methylimidazolium (BMI) with $TFSI^-$ and 600% of BMI with $BF4^-$. Both systems exhibited similar conductivities of 2.3×10^{-3} S/cm at 25 °C. The ability of the PVDF-HFP membrane to retain a large volume of BMI was attributed to its high surface area with an average fiber diameter of < 1 μm, which helped to reduce electrolyte leakage.

Over the last decade, interest in separators with high porosity and high surface area has expanded to aromatic polyimide aerogels. Numerous studies have focused on the synthesis and development of polyimide aerogels having improved mechanical strength, up to 200 MPa [31,32] and excellent thermal stability with onsets of decomposition ranging from 460 °C – 610 °C [31–33] higher than those of ionic liquids [22,23]. Polyimide aerogels are an interesting choice as a porous scaffold that serves as both a battery separator and an electrolyte reservoir due to their high porosity (85% – 95%) and smaller pore sizes. This also improves suppression of lithium dendrites [34,35]. In addition, the high degradation temperature of polyimide aerogels could, in principle, improve battery performance at elevated temperatures, above 300 ºC, for long durations [36–38], thereby decreasing flammability and thermal runaway risks [37,39]. With a wide selection of monomers, the backbone structures of aromatic polyimide aerogels can be tailored to make flexible or rigid substrates [31,37] of varying thicknesses with tunable hydrophobicity and wettability to suit different types of electrolytes, RTILs in particular [34]. Nevertheless, the electrochemical properties of these cross-linked polyimide aerogels have typically been evaluated using electrolytes based on RTILs in mixtures of diethyl carbonate and ethylene carbonate [36,39].

In our previous study, the pore structures of a polyimide gel and its corresponding aerogel composed of the diamine 4,4′-oxydianiline (ODA), the dianhydride biphenyl-3,3′,4,4′-tetracarboxylic dianhydride (BPDA), and the triisocyanate cross-linker Desmodur N3300A were investigated using small-angle neutron scattering (SANS) [40]. The experiment was performed on a polyimide aerogel and on polyimide gels solvated with H_2O, D_2O and three different RTILs (1-ethyl-3-methylimidazolium bis(trifluoromethylsulfonyl)imide, 1-methyl-1-propylpyrrolidinium bis(trifluoromethylsulfonyl)imide, and 1-butyl-1-methylpyrrolidinium bis(trifluoromethylsulfonyl)imide). The data confirmed collapse of some of the polyimide aerogel struts and pores during the supercritical drying process, leading to a lower volume fraction of solvent in the solvated polyimide aerogels when compared to the solvent-exchanged gels.

Herein, we present the development of battery separators based on highly porous polyimide sol-gels that are compatible with several RTILs, resulting in ionic conductivities of up to 10^{-3} S/cm. Based on the SANS results [40] ionic conductivities of six selected imidazolium-based RTILs (Table 1) with 10 wt% lithium bis(trifluoromethanesulfonyl)imide (LiTFSI, $(CF_3SO_2)_2N^-$) salt were screened using the porous ODA/BPDA/N3300A cross-linked gel as the separator. The tetrafluoroborate (BF_4^-) anion was also tested and compared to the most effective RTIL/LiTFSI salt. The effect of separator thickness for the

highly porous and tortuous polyimide gel framework on ionic conductivity and constant current cycling is also discussed.

2. Results and Discussion

The physical, thermal, and morphological properties of ODA/BPDA/N3300A polyimide (PI) gels and aerogels have been well studied [31,40]. Mechanism for the polyimide reaction is as presented in Scheme 1 [40]. Displayed in Fig. 1a is the PI sol-gel film in EMIM/TFSI and LiTFSI solution, and Fig. 1b shows the PI aerogel film after supercritical drying. The cast PI aerogel film was very flexible. The BET surface areas and porosities measured for PI aerogels synthesized in this study were 419 m^2/g and 91% for n = 30, and 344 m^2/g and 87% for n = 60. The thermal stability of the cross-linked PI aerogels was determined using thermogravimetric analysis (TGA) in N_2. There was about a 0.5% weight loss up to 210 °C, indicating a very small degree of incomplete imidization. Although the amount of the cross-linker N3300A in the formulations was small, a slight drop at around 255 °C was likely due to the decomposition of its aliphatic segments [41,42]. The cross-linked polyimide aerogel had an onset decomposition temperature, T_d, of 570 °C with a high char yield (67.6%), as shown in Figure 2a.

Scheme 1. Mechanism for ODA-BPDA based polyimide gel, cross-linked with N3300A (Ref. 40).

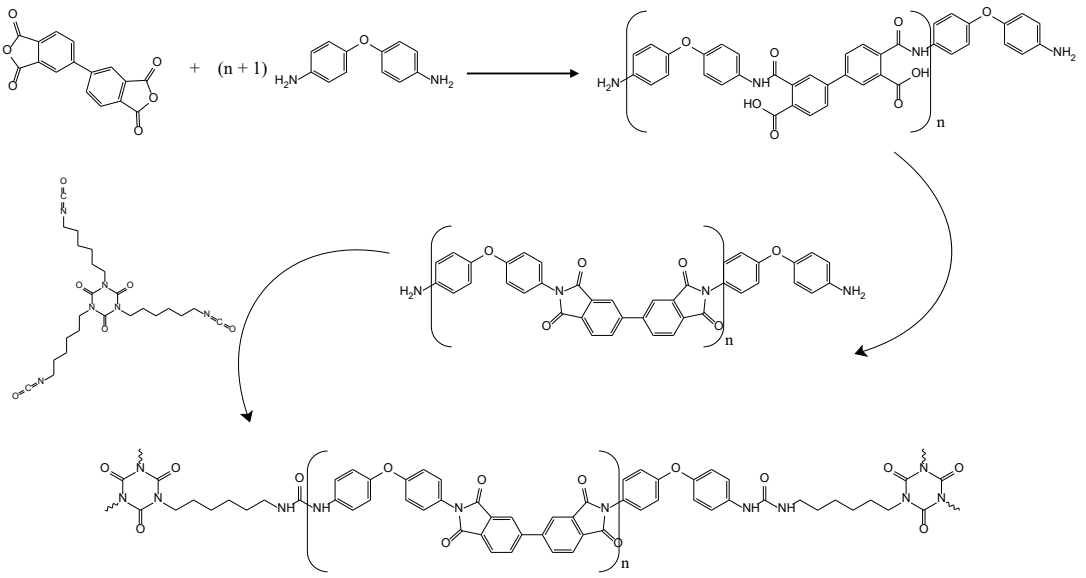

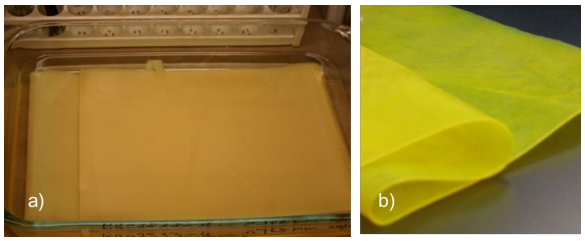

Figure 1. Pictures of a) PI gel film in EMIM/TFSI and LiTFSI solution and b) aerogel film.

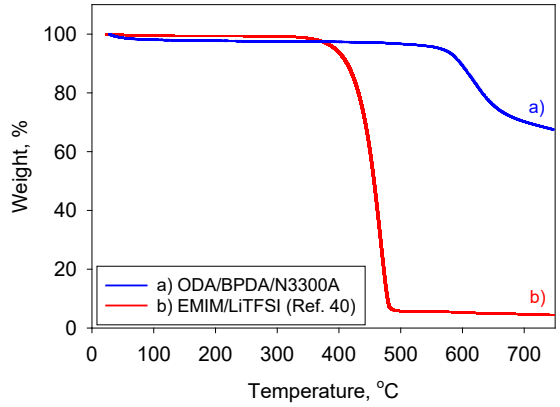

Figure 2. TGA of a) ODA/BPDA/N3300A aerogel with n of 60 and b) EMIM/LiTFSI (Ref. 40) in N_2.

During the film casting process, the exposed top surface of the gel pores partially collapsed and formed a thin skin on the outer surface. In addition, during the supercritical drying process, the PI aerogel underwent some shrinkage due to a reduction of polymer struts [40], further densifying the film surfaces. Figure 3a shows SEM images of the film, highlighting differences between the top side and the pore structure underneath the film surface. Figure 3b shows the SEM image of the film cross-section, and Figures 3c–d (at different magnifications) reveal the retained pore structure underneath the skin layer. Therefore, depending on the thickness of the film, a PI aerogel separator can exhibit different pore volumes and thus different capacities to serve as an ionic liquid reservoir.

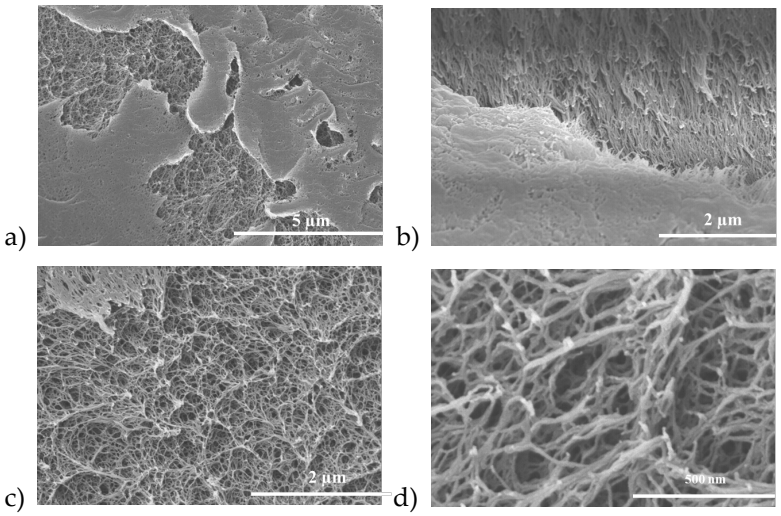

Figure 3. SEM images of a) formation of thin skin on the top surface of the PI aerogel film, b) cross-section of the PI aerogel film, c) and d) pore structures of the PI aerogel underneath the skin layer (at different magnifications).

The hierarchical pore structure formed in the ODA/BPDA/N3300A aerogel was shown to have lower porosity compared to the gel in the solvated state [40]. Hence, the purpose of this study is to examine the impact of the nanopore structure in the polyimide gel separator on lithium-ion transport and conduction using six different room-temperature ionic liquids (RTILs). The ionic liquids in Table 1 were examined in this study with their corresponding salt types, LiTFSI vs. $LiBF_4$.

Shown in Table 2 are 10 experimental runs with polyimide sol-gel films formulated with n = 30 and n = 60, at different film thicknesses, imbibed with RTILs and 10 wt% LiTFSI or $LiBF_4$ and their corresponding ionic conductivities, measured at 25 °C. The imidazolium-based RTILs were selected based on their viscosities, which ranged from 27.9 cP to 56.0 cP, and their ionic conductivities, which ranged from 2.6 mS/cm to 14.1 mS/cm, measured at 20 °C to 30 °C (Table 1). The time required for RTILs with higher viscosities to diffuse into the polyimide gel films was longer than for those with lower viscosities. For instance, it took approximately 2 days or more for RTILs B and C to fully imbibe into the polyimide gel films, while it took one day or less for the others to complete a similar process.

The synthetic route and process to produce for polyimide gel is reported in the Experimental. The complete removal of acetone after solvent exchange with ILs was verified by TGA. Shown in Figure 2c is the TGA plot of 1-ethyl-3-methylimidazolium bis(trifluoromethylsulfonyl)imide (EMIM/TFSI) with 10 wt% LiTFSI after acetone removal. No weight loss attributable to acetone was observed. Only ~0.5 wt% weight loss occurred between 110 °C and 325 °C before the first onset of decomposition of EMIM/TFSI at 370 °C, perhaps due to residual moisture from the LiTFSI.

Table 1. Chemical structure, ionic conductivity, viscosity and density of ionic liquids. Data obtained from IoLiTec, Inc. technical data sheets.

Type	Chemical structure	Ionic conductivity, mS/cm	Viscosity, cP (°C)	Density, g/cm³	Decomposition temperature (°C)
A	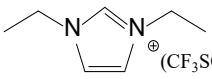 imidazolium bis(trifluoromethylsulfonyl)imide	7.27 (20 °C) 8.24 (30 °C)	27.9 (25°C)	1.45	>200
B	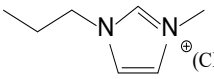 -propylimidazolium bis(trifluoromethylsulfonyl)imide	4.40 (20 °C)	56.0 (19°C)	1.43	N/A
C	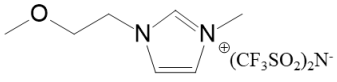 1-(2-methoxyethyl)-3-methylimidazolium bis(trifluoromethylsulfonyl)imide	4.81 (30 °C)	46.9 (25°C)	N/A	N/A
D	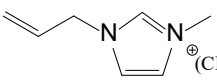 ethylimidazolium bis(trifluoromethylsulfonyl)imide	2.76 (25 °C) 8.87 (30 °C)	35.0 (25°C)	1.49	N/A
E	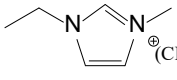 imidazolium bis(trifluoromethylsulfonyl)imide	6.63 (20 °C)	39.4 (20°C)	1.52	250

F	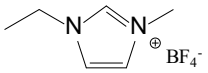 1-ethyl-3-methylimidazolium tetraflouroborate	14.1 (25 °C)	33.8 (25°C)	1.28	N/A

N/A: not available

Ionic conductivities (IC) of the polyimide gel films with n = 30, cast from the same batch, were tested in five ionic liquids A–E (runs 1–5), as reported in Table 2. These ionic liquids had the same anion, $(CF_3SO_2)_2N^-$ ($TFSI^-$), for comparison. Therefore, the differences in ionic conductivities arise mainly from changes in cation interactions with the polyimide gel separator. The commonly used LiTFSI salt was chosen for this study. Figure 4 is a bar chart representing the IC of the neat ILs (data obtained from IoLiTec, Inc. technical data sheets), the measured ICs of the polyimide (PI) gel separator/IL systems, and the corresponding thicknesses of the polyimide gel film separators. Once fully imbibed with ILs, the polyimide gel separators swelled to different thicknesses, suggesting that they absorbed different amounts of IL within their pores and skeletal framework, depending on the chemical structure of the ILs [34]. In general, the ionic conductivity of an RTIL decreases when a Li salt is added, which is in agreement with most ILs tested [24,29,43]. One exception observed was the increase in IC of RTIL D (run 4) upon addition of LiTFSI salt. However, as seen in Figure 4, the differences in thickness of the polyimide gel separators imbibed in RTIL/LiTFSI were relatively small when compared to the percentage loss of IC. Thus, this suggests that there is a chemical and/or phase interaction between the polyimide gel separator and these ionic liquids complexed with LiTFSI salt. This behavior warrants further investigation.

Table 2. Screening results of ionic conductivity of polyimide sol-gels with different repeating unit, n, and thicknesses in various ILs.

Run #	RTIL Type	n	Ionic conductivity of RTIL solvated PI gel (mS/cm)	Loss in ionic conductivity (%)	Film thickness of RTIL solvated PI gel (cm)
1[a]	**A**	30	4.19	(-) 42.4	0.0774
2[a]	**B**	30	1.49	(-) 66.2	0.0738
3[a]	**C**	30	2.37	(-) 50.7	0.0702
4[a]	**D**	30	3.91	(+) 41.7	0.0834
5[a]	**E**	30	5.57	(-) 16.0	0.0742
6[b]	**E**	60	3.23	(-) 51.3	0.0158
7[b]*		60	2.84	(-) 57.2	0.0158
8[c]		60	2.54	(-) 61.7	0.0087
9		60	1.69	(-) 74.5	0.0036

10[c]	**F**	60	3.76	(-) 73.3	0.0076

[a] From same batch of film cast with n = 30

[b] From same batch of film cast with n = 60

[b*] Ionic conductivities measured 4 months after preparation

[c] From same batch of film cast with n = 60

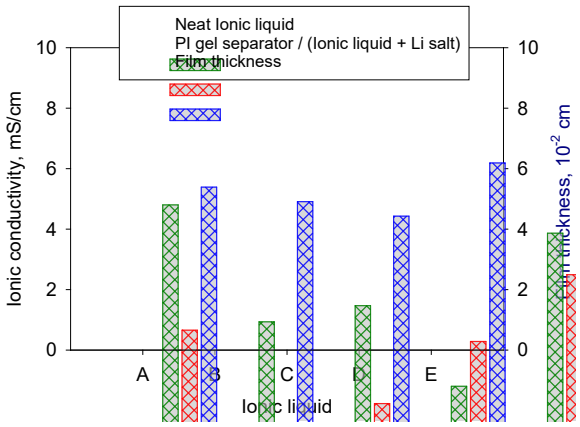

Figure 4. Comparison of neat ILs and IL + Li salt/PI gel separators and gel film thickness measured at room temperature (25 °C). Specimens were from the same batch of gel film cast with the same initial thickness and n = 30 (runs 1–5).

Based on the ionic conductivity performance from experiments 1–5, it was determined that the polyimide gel separator with RTIL-E complexed with 10 wt% LiTFSI demonstrated the best combination of properties for coin-cell performance testing (Figure 5). The two dominant factors determining ionic conductivity within the PI gel separators are the film thickness and the pore structure within the gel. This claim was further evaluated by examining three additional polyimide gel films with n = 60 and thicknesses of 158 μm (run 6), 87 μm (run 8), and 36 μm (run 9). Each gel film was fully imbibed with ionic liquid E and 10 wt% LiTFSI.

All data were analyzed using Design-Expert software. The results suggested that the separator thickness had a significant effect on ionic conductivity (R^2 = 0.9451, standard deviation = 0.3935), as shown in Figure 5, whereas the backbone chain length (n) did not. As the thickness of the gel film decreased from 745 μm to 36 μm, a drop in IC was observed, from (−)16% down to (−)74.45% (Table 2, runs 5–9). The skin that formed on top of the gel film may have contributed to this drop as a result of partial blockage of ion transport between the two electrodes. Note that ion-transporting channels between these separators can change as a function of surface area and porosity.

An additional experiment was performed to measure the ionic conductivity of a separator with a thickness of 158 μm, fully imbibed with ionic liquid E, after 4 months in storage (run 7). The results showed a slight drop in ionic conductivity, from 3.23 mS/cm (run 6) to 2.84 mS/cm (run 7). The decrease in IC was most likely due to moisture absorption.

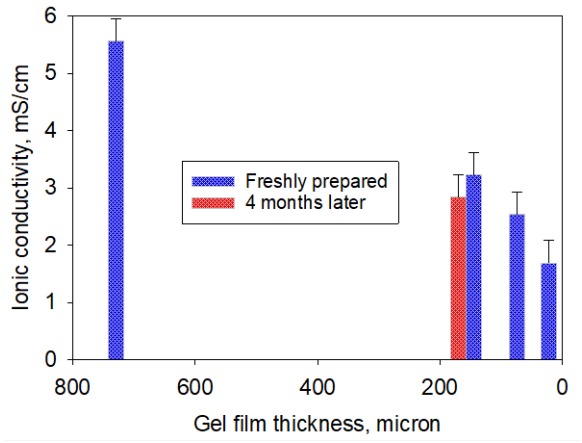

Figure 5. Ionic conductivity of EMIM/LiTFSI (RTIL-E) in polyimide gel separators of different thicknesses (blue bars) and corresponding IC on a PI gel separator after 4 months (red bar) (R^2 = 0.9451, std. dev. = 0.3935).

Similar to RTIL-E (EMIM/TFSI), which uses bis(trifluoromethylsulfonyl)imide ($TFSI^-$) as an anion, the ionic liquid EMIM/BF_4 with tetrafluoroborate (BF_4^-) as an anion (RTIL-F) is also of interest in several studies, perhaps due to its higher IC and lower viscosity [24,40]. As seen in Table 1 and presented in Figure 6, EMIM/BF_4 has the highest ionic conductivity among all ILs examined. When tested with the polyimide sol-gel film as the separator, RTIL-F (run 10) exhibited higher ionic conductivity than RTIL-E (run 8), 3.76 mS/cm vs. 2.54 mS/cm, despite its larger drop from the initial neat-IL value, (−)73.3% vs. (−)61.7%, respectively. Based on the film thicknesses (Table 2), it is interesting to note that the PI gel film separator imbibed with EMIM/TFSI (run 8) was thicker than that with EMIM/BF_4 (run 10). This observation is in agreement with results found by Cheruvally et al [30].

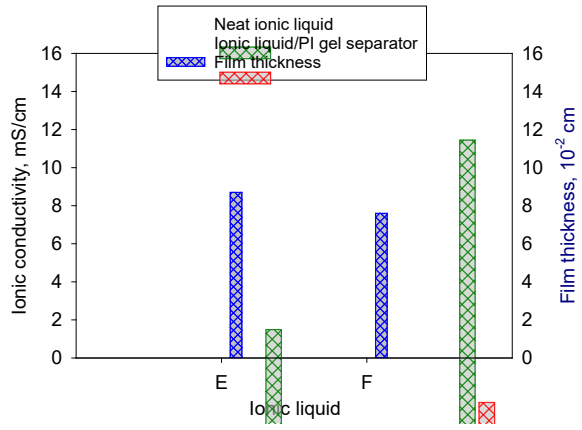

Figure 6. Comparison of neat EMIM/TFSI (RTIL-E) and EMIM/BF_4 (RTIL-F) and their corresponding RTIL/PI gel separators and gel film thickness measured at room temperature (25 °C). Specimens were from the same batch of gel film cast with the same initial thickness and n = 60.

Coin cells with active carbon as positive electrode, Li metal as negative electrode and PI gel imbibed with RTIL/LiTFSI salt serving as dual function of separator and electrolyte were fabricated and tested under constant current cycling. Additional coin cells were

tested to elucidate differences between PI gels imbibed with ionic liquid solutions E and F (Figure 7). The cells were charged up to 4.5 V and then discharged to 2.0 V at a rate of 50 mA/g. The response curves of voltage (red) vs. constant current (blue are plotted in Figure 7. As seen in Figure 7a, the coin cells with PI gel imbibed with EMIM/TFSI+LiTFSI salt cycled well. However, those with PI gel imbibed with EMIM/BF4 +LiTFSI salt showed a depressed voltage profile and the voltage dropped immediately after the initial discharge, as shown in Figure 7b. This phenomenon indicates that the rapid voltage drop was caused by contact/cell internal resistance (IR). A possible reason is the incompatibility of the BF_4^- anion with Li metal, forming a resistive layer on the Li metal surface.

Displayed in Figure 8 are pictures of the lithium metal foils dipped in EMIM/TFSI (Fig. 8a) and EMIM/BF_4 (Fig. 8b). While EMIM/TFSI remained clear and Li metal was stable over time, the EMIM/BF_4 ionic liquid changed color and became progressively more yellow after 24 h. This could explain the voltage decay due to decomposition at the Li metal surface in the EMIM/BF_4 solution. This perceptible reaction merits further investigation.

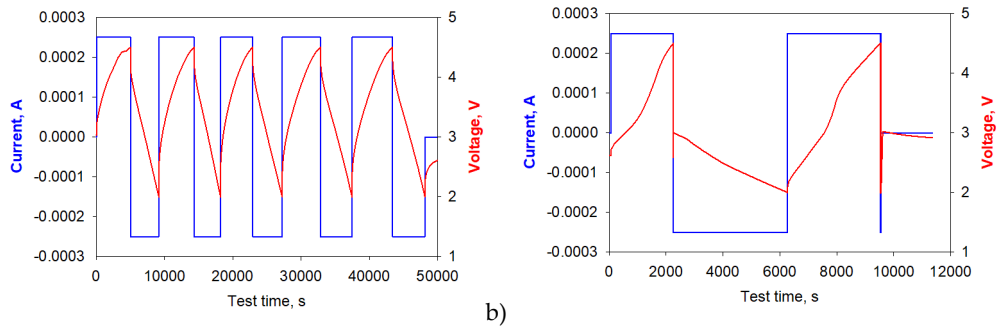

a) b)

Figure 7. Cycling tests of coin cells with polyimide gels imbibed with IL/Li salt as separators: (a) EMIM/TFSI and (b) EMIM/BF_4.

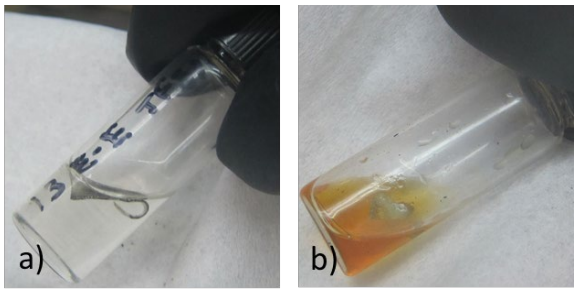

Figure 8. Li metal foils soaking in a) EMIM/TFSI and in b) EMIM/BF_4.

3. Conclusions

A polyimide gel separator based on BPDA/ODA/N3300A has been successfully synthesized and was evaluated by imbibed with six RTIL conducting electrolytes comprising imidazolium cations with 10 wt% LiTFSI salt. These RTIL/TFSI-solvated PI gels demonstrated ionic conductivities over 1×10^{-3} S/cm, in the range suitable as a replacement for current standard polyolefin microporous membranes. Furthermore, the polyimide sol-gel materials exhibit onset decomposition temperatures of ~570 °C. The ionic conductivity and constant current cycling performance of room-temperature ionic liquid

E, EMIM/TFSI, were found to be the best among the systems examined for this polyimide gel separator. The ionic conductivity decreased as the thickness of the polyimide gel separator decreased in these experiments, consistent with the presence of a surface skin and changes in effective transport pathways. The anion type, $TFSI^-$ vs. BF_4^-, also played a key role in ionic conductivity as well as in the electrochemical stability of the system with this polyimide gel separator.

The preparation and use of this sol-gel were also advantageous in that they allowed us to bypass the time-consuming supercritical CO_2 extraction needed to create dry aerogels. Another favorable feature of this direct RTIL penetration procedure is the elimination of additional wetting components such as carbonate solvents.

4. Materials and Methods

4.1. Materials

The diamine 4,4′-oxydianiline (ODA) was purchased from Wakayama Seika Kogyo Co., Ltd. The dianhydride biphenyl-3,3′,4,4′-tetracarboxylic dianhydride (BPDA) was purchased from UBE America, Inc. The trifunctional cross-linker, triisocyanate Desmodur N3300A, was purchased from Bayer Material Science. N-methylpyrrolidone (NMP) was purchased from Tedia. Acetic anhydride (AA), triethylamine (TEA), lithium bis(trifluoromethanesulfonyl)imide (LiTFSI) salt, Li metal, and polyvinylidene fluoride (PVDF) were all purchased from Sigma-Aldrich. Acetone was purchased from Fisher Chemical. The high surface area active carbon powder was purchased from MTI. Six imidazolium-based RTILs with relatively low viscosities used in the experiments were obtained from IoLiTec, Inc. Chemical structures of these ionic liquids and their properties are presented in Table 1. The dianhydride BPDA was vacuum dried at 135 °C overnight prior to synthesis, and the active carbon was dried at 100 °C under vacuum overnight before use. All other reagents were used as received with no further purification.

4.2. Preparation of Polyimide Gels

The polyimide gel was formulated as described in our previous investigations [31,40]. The backbone of the polyimide aerogel was synthesized with n equivalents of the dianhydride BPDA and n+1 equivalents of the diamine ODA, then cross-linked with the trifunctional isocyanate monomer N3300A to form a three-dimensional network. The polyimide backbone chain length was formulated with n = 30 and n = 60 between cross-links. The reaction was carried out in the polar aprotic solvent NMP and chemically imidized at room temperature using acetic anhydride (AA) as a water scavenger and triethylamine (TEA) as a catalyst.

The synthesis for n = 60, for example, is as follows: BPDA (3.15 g, 10.7 mmol) was added to a solution of ODA (2.18 g, 10.9 mmol) in 38.8 mL of NMP. The mixture was stirred for 15 minutes until homogeneous. Acetic anhydride (8.10 mL) and TEA (3.0 mL) were added sequentially and stirred for ten minutes. Next, N3300A (0.060 g, 0.119 mmol), dissolved in 5 mL NMP, was added. The mixture was stirred for another 10 minutes before being cast into a thin film. This thin gel film was then aged for 12–18 hours at room temperature in a closed container. The gel film, still in NMP, was then washed with a 50/50 volume-percent mixture of NMP/acetone followed by four subsequent washes with acetone. Both the thin polyimide gel films with n = 30 and n = 60 were stored in acetone until

they were ready for solvent exchange with RTILs or supercritical drying to produce polyimide aerogels.

It is important to reduce the thickness of the separator as much as possible since the thickness of the internal components within a cell has a dramatic effect on the specific energy of the battery. Although the ODA/BPDA/N3300A-based gel film formulation was castable, obtaining thinner films depended strongly on the viscosity of the polyamic acid solution. For example, the viscosity of a cross-linked polyamic acid solution with n = 30 remained low for ~10 minutes after the cross-linker N3300A was added, but increased rapidly as the gelation point was approached, making it difficult to cast a film larger than 2.5 in. × 5 in. Our preliminary work showed that a more controllable viscous solution could be achieved by formulating a gel with a longer chain length, thus limiting the amount of spreading during film casting. With n = 60, the viscosity was consistent for at least 15 minutes after the cross-linking reaction started, providing a larger processing window to produce a 1-foot by 10-foot sheet of gel film from a continuous cast on a pilot scale.

4.3. Properties of Polyimide Aerogel Films

The polyimide aerogel film was obtained using a supercritical CO_2 extraction method. Any residual solvent in the aerogel films was removed by further outgassing in an oven at 80 ºC overnight under full vacuum. Brunauer–Emmett–Teller (BET) surface area data were obtained from a Micromeritics ASAP 2020 chemisorption apparatus. Morphologies of the aerogel films were examined using a Hitachi S-4700-11 field emission scanning electron microscope. The percent porosity was calculated from the measured bulk density (ϱb) and skeletal density (ϱs) using equation (1):

$$\text{Porosity (\%)} = (1 - \varrho b/\varrho s) \times 100\% \quad (1)$$

4.4. Preparation of Electrolyte Solvated Polyimide Gels

The ionic liquid (IL) solution with 10 wt% LiTFSI salt (0.5289 M) was prepared in a humidity-controlled dry room and mixed at room temperature overnight. The IL/Li salt mixture was then added directly to the acetone-saturated polyimide gel film. The films initially floated on the top layer because of the differences in density and viscosity between the IL/Li salt solution and acetone. The gel film slowly sank to the bottom of the container over a period of one to three days, indicating that the gel was saturated with the electrolyte. The acetone was then removed by allowing the open container to stand in air for 48 hours, permitting the acetone to evaporate and leaving only the polyimide gel imbibed with the IL/Li salt.

4.5. Preparation of Electrodes and Fabrication of Lab Cells

The active carbon, Super P carbon, and PVDF were dry mixed in a weight ratio of 90:5:5. Next, NMP (with PVDF:NMP at ~1:50 by weight) was added to the well-mixed powder. The mixture was stirred at 800 rpm overnight to ensure that the slurry was homogeneous. The prepared slurry was cast on an aluminum foil substrate to a typical thickness of 5 mils. The aluminum foil coated with the slurry was dried at 70 ºC under a hood. The remaining NMP was removed in an oven at 110 ºC overnight under a full vacuum.

The dried cathode/electrode described above, Li metal anode, and the polyimide gel imbibed with RTIL/Li salt as a separator were assembled and crimped into lab cells, i.e., coin cells (2325), in an Ar-filled glove box located in a dry room. The fabricated coin cells were then subjected to electrochemical cycling tests.

4.6. Ionic Conductivity Measurement

The ionic conductivity (σ, in S cm^{-1}) of the electrolyte-solvated polyimide gels was determined using electrochemical impedance spectroscopy (EIS) at room temperature. The prepared RTIL-solvated polyimide gel was first cut into 0.5-inch diameter round samples (area A = 1.266 cm^2). Any electrolyte outside the gel was wiped off using Kimwipes, and then the thickness (L) of the gel film was measured. The gel film was sandwiched between two stainless steel (SS) blocking disks with a diameter of 0.5 inches. Pressure was applied to ensure good contact between the gel film and the two SS electrodes (SS | polyimide gel film | SS). EIS was then measured using a Solartron SI-1287 potentiostat in combination with a Solartron 1255B frequency response analyzer in the frequency range of 10^6 – 1 Hz with a 10 mV AC amplitude perturbation. The data were plotted in Nyquist form, and the overall resistance of the polyimide gel film (R_{bulk}) was determined from the intercept of the semicircle with the real axis, Z_{real}. The σ of the polyimide gel samples was calculated based on the thickness (L, in cm), surface area (A, in cm^2), and R_{bulk} (Ω) using equation (2):

$$\sigma = L / (R_{bulk} \times A) \quad (2)$$

Author Contributions: Concept, design, experimental performance and data curation,: B.D., P.L., R.P.V, J.W. and B.N.N.; thermal analyses: D.A.S.; writing (original draft): B.N.N.; Review and editing: R.P,V.; J.W. and D.A.S. All authors have read and agreed to the published version of this manuscript.

Funding: This work was supported through the Multifunctional Structures with High-Energy Lightweight Loading-Bearing Storage (M-SHELLS) project as a part of the Convergent Aeronautics Solution (CAS) execution project under NASA Transformative Aeronautics Concepts Program.

Institutional Review Board Statement: Not applicable.

Informed Consent Statement: Not applicable.

Data Availability Statement: The original contributions presented in this study are included in the article.

Acknowledgments: The authors thank Haiquan Guo for the BET data and Linda McCorkle for the SEM images.

Conflicts of Interest: The authors declare no conflicts of interest.

References

1. Zhang, S. S. A Review on the Separators of Liquid Electrolyte Li-ion Batteries. *J. Power Sources* **2007**, *164*, 351-364.
2. Lee, H.; Yanilmaz, m.; Toprakci, O.; Fu, K.; Zhang, X. A Review of Recent Developments in Membrane Separators for Rechargeable Lithium-Ion Batteries. *Energy Environ. Sci.* **2014**, *7*, 3857-3886.
3. Choudhury, S; Azizi. M.; Raguzin, I.; Göbel, M.; Michel, S.; Simon, F.; Willomitzer, A.; Mechtcherine, V.; Stamm, M.; Ionov, L. Effect of fibrous separators on the performance of lithium–sulfur batteries. *Phys. Chem. Chem. Phys.* **2017**, *19*, 11239-11248.

4. Cannarella, J.; Liu, X.; Leng, C. Z.; Shiko, P. D.; Gor, Y.; Arnold, C. B. Mechanical Properties of a Battery Separator under Compression and Tension. *J. Electrochem. Soc*. **2014**, *161*, F3117-F3122.
5. Scrosatti, B. Recent Advances in Lithium Ion Battery Materials. Electrochimica Acta **2000**, *45*, 2461-2466.
6. Liu, K.; Liu, Y.; Lin, D.; Pei, A.; Cui, Y. Materials for lithium-ion battery safety. *Sci. Adv*. **2018**, *4*, eaas9820.
7. Francis, C. F.; Kyratzis, I. L.; Best, A. S. Lithium-ion Battery Separators for Ionic-liquid Electrolytes: A Review. *Adv. Mater*. **2020**, *32*, 1904205.
8. Chen, W.; Wang, X.; Liang, J.; Chen, Y.; Ma, W.; Zhang, S. A High Performance Polyacrylonitrile Composite Separator with Cellulose Acetate and Nano-Hydroxyapatite for Lithium-Ion Batteries. *Membranes*, **2022**, *22*, 124.
9. Kang, S. H.; Jang, J-K,; Jeong, H. Y.; So, S.; Hong, S-K.; Hong, Y. T.; Yoon, S. J.; Yu, D. M. Polyacrylonitrie/Phosphazene Composite-Based Heat-Resitant and Flame-Retardant Separators for Safe Lithium-Ion Batteries. *ACS App. Energy Mater*. **2022**, *5 (2)*, 2452-2461.
10. Arifeen, W. U.; Kim, M.; Ting, D.; Kurniawan, R.; Choi, J.; Yoo, K.; Ko, T. H. Hybrid thermal resistant electrospun polymer membrane as the separator of lithium ion batteries. *Mater. Chem. Phy*. **2020**, *245*, 122780.
11. Liu, R., Yuan, B.; Zhong, S.; Liu, J.; Dong, L.; Ji, Y.; Dong, Y.; Yang, C.; He, W. Poly(vinylidene fluoride) separators for next-generation lithium based batteries. *Nano Select* **2021**, *2*, 2308.
12. Dallaev, R.; Pisarenko, T.; Sobola, D.; Orudzhev,F.; Ramazanov, S.; Trčka, R. Brief Review of PVDF Properties and Applications Potential. *Polymers* **2022**, *14* (22), 4793.
13. Mahant, Y. P.; Kondawar, S. B.; Nandawar, D. V.; Kohnkar, P. Poly(methyl methacrylate) reinforced poly(vinylidene Flourinde) composites electrospun nanofibrous polymer electrolyes as potential separator for lithium ion batteries. *Mater. Renew*. Sus Ener. **2018**, *7*, 5.
14. Zhang, H.; Zhang, Y.; Xu, T.; John, A. E.; Li, Y.; Li, W.; Zhu, B. Poly(m-phenylene isophthalamide) separator for improving the heat resistance and power density of lithium-ion batteries. *J. Power Sources* **2016**, *329*, 8-16.
15. Lin, G.; Bai, Z.; Liu, C.; Liu, S.; Han, M.; Huang, Y.; Liu, X. Mechanically robust, noflammable and surface crss-linking composite membranes with high wettability for dendrite-proof and high-safely lithium-ion batteries. *J. Membrane Sci*. **2022**, *647*, 120262.
16. Branco, L. C.; Rosa, J. N.; Ramos, J. J. M.; Afonso, C. A. M. Prepration and Characterization of New Room Temperature Ionic Liquids. *Chem. Eur. J.* **2002**, *8 (6)*, 3671-3677.
17. Hapiot, P.; Lagrost, C. Electrochemical Reactivity in Room-Temperature Ionic Liquids. *Chem. Rev*. **2008**, *108*, 2238-2264.
18. Chen, Y,; Liu, S.; Bi, Z.; Li, Z.; Zhou, F.; Shi, R.; Mu, T. Reviewing electrochemical stability of ionic liquids-/deep eutectic solvents-based electrolytes in lithium-ion, lithium-metal and post-lithium-ion batteries for green and safe energy. *Green Energy Environ*. **2024**, *9*, 966-991.
19. Park, J.; Jung, Y.; Kusunah, P.; Lee, J.; Kwon, K.; Lee, C. K. Application of Ionic Liquids in Hydrometallurgy. *Int. J. Mol. Sci*. **2014**, *15*, 15320-15343.
20. Murugesan, S.; Linhardt, R. J. Ionic Liquids in Carbohydrate Chemistry – Current Trends and Future Direction. *Current Org. Synt*. **2005**, *2*, 437-451.
21. Tang, X.; Lv, S.; Jiang, K.; Zhou, G.; Liu, X. Recent development of ionic liquid-based electrolytes in lithium-ion batteries. *J. Power Sources* **2022**, *542*, 231792.
22. Ngo, H. L.; LeCompte, K.; Hargens, L.; McEwen, A. B. Thermal Properties of Imidazolium Ionic Liquids. *Thermochimica Acta* **2000**, *357-358*, 97-102.
23. Xu, C.; Cheng, Z. Thermal Stability of Ionic Liquids: Current Status and Prospects for Future Development. *Process* **2021**, *9 (12)*, 337.
24. Huie, M. M.; DiLeo, R. A.; Marschilok, A. C.; Takeuchi, K. J.; Takeuchi, E. S. Ionic Liquids Hybrid Electrolytes for Lithium-Ion Batteries: A Key Role of the Separator-Electrolyte Interface in Battery Electrochemistry. *ACS Appl. Mater. Interfaces*, **2015**, *7*. 11724-11731.
25. Kirchhöfer, M.; von Zamory, J.; Paillard, E.; Passerini, S. Separators for Li-Ion and Li-Metal Battery Including Ionic Liquid Based Electrolytes Based on $TFSI^-$ and FSI^- Anions. *Int. J. Mol. Sci*. **2014**, *15*, 14868-14890.
26. Evans, T.; Lee, J-H.; Bhat, V.; Lee, S-H. Electrospun Polyacrylonitrile Microfiber Separators for Ionic Liquid Electrolytes in Li-Ion Batteries. *J. Power Sources* **2015**, *292*, 1-6.
27. Sun, Y.; Wang, J.; Prausnitz, J. Interfacial properties between ionic-liquid-based electrolytes and lithium-ion-battery separator. *AlChE J*. **2021**, *67*, e1708.
28. Caimi, S.; Klaue, A.; Wu, H.; Morbidelli, M. Effect of SiO2 Nanoparticles on the Performance of PVdF/-HFP/Ionic Liquid Separator for Lithium-Ion Batteries. *Nanomaterials* **2018**, *8*, 926.

29. Eftekhamia, M.; Hasanpoor, M.; Forsyth, M.; Kerr, R.; Howlett, P. Toward Practical Li Metal Batteries: Importance of Separator Compatibility Using Ionic Liquid Electrolytes. ACS *Appl. Ener. Mater* **2019**, *2 (9)*, 6655-6663.
30. Cheruvally, G.; Kim, J-K.; Choi, J-W.; Ahn, J-H.; Shin, Y-J.; Manuel, J.; Raghavan, P.; Kim, K-W.; Ahn, H-J.; Choi, D. S.; Song, C. E. Electrospun Polymer Membrane Activated with Room Temperature Ionic Liquid: Novel Polymer Electrolytes for Lithium Batteries. *J. Power Sources*, **2007**, *172*, 863-869.
31. Nguyen, B. N., Meador, M. A. B., Scheiman, D., McCorkle, L. Polyimide Aerogels Using Triisocyanate as Cross-linker. *ACS Appl. Mater. Interfaces* **2017**, *9*, 27313-27321.
32. Nguyen, B. N.; Scheiman, D.; Meador, M. A. B.; Guo, J.; Hamilton, B.; McCorkle, A. Effect of Urea Links in the Backbone of Polyimide Aerogels. *Appl. Polym. Mater*. **2021**. *3 (4)*, 2027-2037.
33. Zheng, S.; Jiang, L.; Chang, F.; Zhang, C.; Ma, N.; Liu, X. Mechanically Strong and Thermally Stable Chemical Cross-Linked Polyimide Aerogels for Thermal Insulator. *ACS Appl. Mater. Interfaces* **2022**, *14*, 50129-50141.
34. Deng, Y.; Pan, Y.; Li, C.; Zhang, Z.; Gong, L.; Fu, Y.; Shi, L; Zhang, H.; Cheng, X. Advanced Polyimide Separator Via Co-precursor Method for Lithihm-ion Batteries with Low Thermal Runaway Risks. *J. Energy Storage*, **2022**, *56: Part B*, 106100.
35. Ding, L; Yue, X.; Zhang, X,; Chen, Y.; Liu, J.; Shi, Z.; Wang, Z.; Yan, X.; Liang, Z. A polyimide aerogel separator with electron cloud design to boost Li-ion transport for stable Li metal batteries. *PNAS* **2023**, *120 (51)*, e2314264120.
36. Deng, Y.; Pan, Y.; Zhang, Z.; Fu, Y.; Gong, L.; Liu, C.; Yang, J.; Zhang, H.; Cheng, X. Novel Thermotolerant and Flexible Polyimide Aerogel Separator Achieving Advanced Lithium-Ion Batteries. *Adv. Funct. Mater.* **2022**, *32 (4)*, 2106176.
37. Wei, H.; Hu, X.; Deng, Y.; Wei, X.; Yang, Z.; Han, G. Distributed activation energy treatment of polyimide aerogel and its blocking effect on thermal runaway propagation of ternary battery. *J. Ener. Storage* **2024**, *90*, 111744.
38. Wang, Y.; Zhou, K.; Cui, L.; Mei, J.; Li, S.; Li, L.; Fan, W.; Zhang, L.; Liu, T. Ion transport regulation of polyimide separator for safe and durable Li-metal battery. *J. Power Sources* **2024**, *591*, 233853.
39. Shi, J.; Hu, H.; Xia, Y.; Liu, Y.; Liu, Z. Polyimide matrix-enhanced cross-linked gel separator with three-dimensional heat-resistance skeleton for high-safety and high-power lithium ion batteries *J. Mater. Chem. A* **2014**, *2*, 9134.
40. Rinehart, S. J.; Nguyen, B. N.; Viggiano, R. P.; Meador, M. A. B.; Dadmum, M. D. Unexpexted Hierarchical Porosity in Polyimide Aerogels and Corresponding Solvated Gels. *ACS Appl. Mater. Interfaces* **2020**, *12*, 30457-30465.
41. Czlonka, S.; Bertino, M. F.; Kośny, J.; Shukla, N. Density and shrinkage as guiding criteria for the optimization of the thermal conductivity of poly(urethane)-glass aerogels. *J. Sol. Sci. Tech.* **2020**, *93*,149-167.
42. Data obtained from Covestro Safety Data Sheet
43. Hayamizu, K.; Tsuzuki, S.; Seki, S. Transport and Electrochemical Properties of Three Quaternary Ammonium Ionic Liquids and Lithium Salts Doping Effect Studied by NMR Spectroscopy. *J. Chem. Eng. Data* **2014**, *59*, 1944-1954.